Gazi University Journal of Science
Part A: Engineering And Innovation
GU J Sci Part:A
2(1):77-85 (2014)

Modeling And Analysis of A Jeffcott Rotor As A Continuous Cantilever Beam And An Unbalanced Disk System

O. GUNDOGDU[1, ♠] , K. ALNEFAIE[2] , H. DIKEN[2]

[1] *Ataturk University, Faculty of Engineering, Mechanical Engineering Department, 25240 Erzurum, TURKEY*

[2] *King Abdulaziz University, Faculty of Engineering, Mechanical Engineering Department, P.O. Box 80204, Jeddah 21589, SAUDI ARABIA*

Received:09.02.2013 Accepted:19.03.2014

ABSTRACT

The paper presents simulations of a continuous cantilever beam and an unbalanced disk system by extending classical Jeffcott rotor approach to a model that gives the first three (or more) modes of the flexible beam. Normal modes of a constrained structure method are used to develop the equations of motion including gyroscopic effects. Centrifugal force created by the unbalanced mass of the disk is considered as a constraint for the flexible beam. The first three modes of the flexible beam having an unbalanced disk are taken into consideration, which cannot be found through the classical Jeffcott rotor modeling. Hence, the model computes the first three natural frequencies of the rotor, and presents a very good correspondence with the first natural frequency obtained by the Jeffcott model. The change in the natural frequencies with respect to the disk mass to shaft mass ratio and the disk diameter to shaft length ratio are computed and presented. Instability problem due to inertial effects is encountered if these two ratios are kept high; which cannot be predicted by the classical Jeffcott rotor model.

Key words: Jeffcott rotor, rotor whirl, modal vibration.

1. INTRODUCTION

Unbalanced masses are the main causes of the vibration in rotating machinery. Rankine (1869) is credited as being the first to realize the influence of unbalance on rotating shafts, which is the main source of centrifugal forces in such systems. These forces cause large whirl amplitudes when the shaft is rotated at its natural frequency, which is also called as critical speed. Foppl (1895) modeled the rotor as a single disk centrally located on a shaft without damping while Jeffcott (1919) studied the same model with damping, and rotors modeled in this fashion are called Jeffcott rotor models [1-3].

The approaches to establish models for rotordynamics vary in the literature, and it is beyond the scope of this work to give a detailed portrait of the modeling

♠Corresponding author, e-mail: omergun@atauni.edu.tr

methodologies present. Instead, several approaches will be cited here, and the interested reader should refer to references [4-8]. For instance, Genta [9] used the finite element method based on complex coordinates to investigate the whirling of unsymmetrical rotors for a general multi degree of freedom rotor, and resulted in a simpler set of equations and hence had advantages in simulations of undamped axisymmetrical systems. Kessler [10] developed a method involving complex modal analysis to investigate rotating systems, where the natural mode of the rotor was assumed to be the sum of sub-modes rotating in opposite directions. In that way, complex analysis of free and forced vibration of anisotropic systems was realized. Campos et al. [11], on the other hand, developed a Jeffcott model using bond graphs method based on Lagrange, compared the model with Hamilton's method, and concluded that the bond graph approach requires less tedious work and can be applied to more complex systems. Lately, Khanlo et al. [12] modeled a rotating flexible continuous shaft-disk system with assumed modes method to analyze chaotic vibration due to rub-impact.

Although a vast amount of research on Jeffcott model exists in the literature, the continuous beams in their models are unfortunately considered with their equivalent stiffness or elasticity but with the first mode only. In this study, however, the method is further extended to a system where Jeffcott rotor model is considered as a disk supported by a continuous flexible cantilever beam (shaft). The first three modes of the continuous shaft are taken into account as opposed to the classical Jeffcott rotor, which gives only the first mode approximately. The equations are developed accordingly by using normal modes of a constraint structure method including gyroscopic effects. Eigenvalue analysis is performed with respect to the disk-mass to shaft-mass ratio and for disk-diameter to shaft-length ratio. Consequently, this paper extends the classical Jeffcott model to a new one that makes possible to compute more than one mode of vibration by assuming a flexible beam in its model.

2. FORMULATION

Figure 1 shows a Jeffcott rotor model on a cantilever flexible beam with a thin disk at the tip. The shaft has a length of L and diameter of d, while the thin disk has a diameter of D.

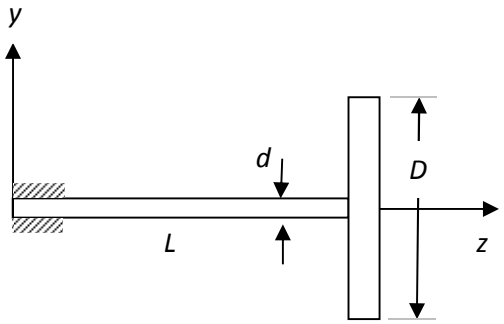

Figure 1. Jeffcott rotor supported by a cantilever flexible beam.

Figure 2 shows the side-view of the rotating disk in whirl, where the inertial coordinate axes and the rotating coordinate axes attached to the disk are respectively shown as OXY and Oxy. The letter S on the disk represents the geometric center, G the mass center of the disk, $OS=r$ the whirl radius, $SG=e$ the mass eccentricity, m_d the disk mass, ψ the disk rotation angle, θ the whirl angle.

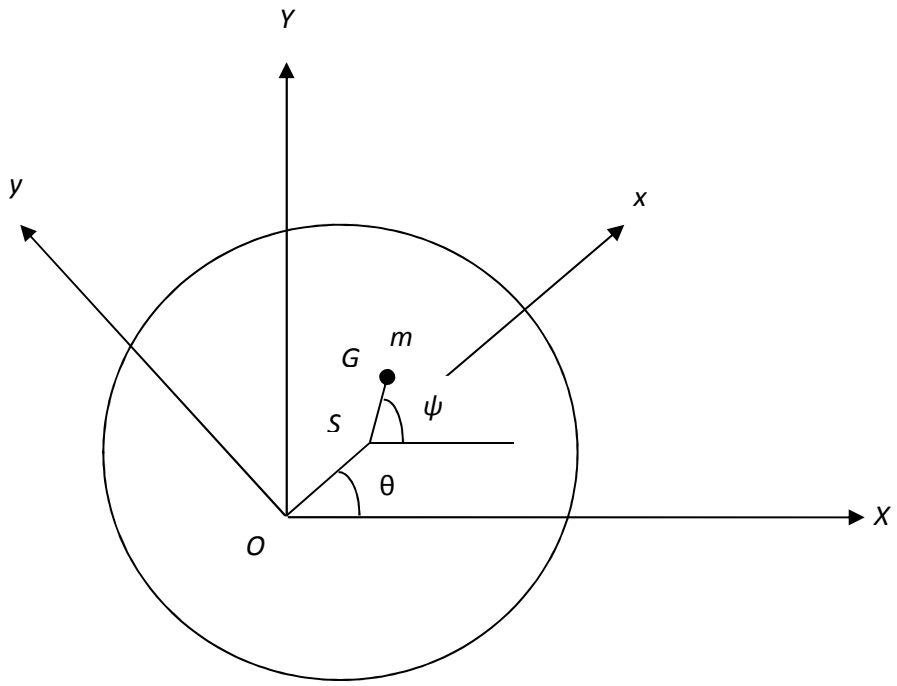

Figure 2. Side view of the rotating disk.

The dynamic equations of the motion are obtained via the method of normal modes of constrained structures [13]. Deflection of the flexible beam in x and y directions can be written in terms of an orthogonal modes as

$$x(z,t) = \sum_i \phi_i(z)\, q_{xi}(t) \quad (1)$$

$$y(z,t) = \sum_i \phi_i(z) q_{yi}(t) \quad (2)$$

where q_i is the ith generalized coordinate and ϕ_i is the ith orthogonal mode.

Kinetic energy of the shaft in y direction can be expressed as

$$T = \frac{1}{2}\int_0^L \dot{y}^2(z,t) m_s(z) dz = \frac{1}{2}\sum_i M_i\, \dot{q}_{yi}^2 \quad (3)$$

The generalized masses are then defined as

$$M_i = \int_0^L \phi_i^2(z) m_s(z) dz = m_s \int_0^L \phi_i^2(z) dz \quad (4)$$

Here m_s is the shaft mass per unit length which is assumed constant, while the potential energy of the shaft in y direction is

$$U = \frac{1}{2}\int_0^L EI y''^2(z,t)\, dz = \frac{1}{2}\sum_i K_i q_{yi}^2 \quad (5)$$

The generalized stiffness in this equation is defined as

$$K_i = \int_0^L EI \phi_i''^2(z) dz \quad (6)$$

where EI is the shaft rigidity. If there is concentrated force or moment acting at the tip of the beam, the generalized force can then be found by the principle of virtual work.

If Lagrange equation is used and viscous damping is assumed for the elastic beam, then the equations for the generalized coordinates in the x and y directions can be obtained as follows;

$$\ddot{q}_{xi} + 2\zeta_i\omega_i\dot{q}_{xi} + \omega_i^2 q_{xi} = \frac{1}{M_i}\left[F_x(L,t)\phi_i(L) + M_y(L,t)\phi'_i(L)\right] \quad (7)$$

$$\ddot{q}_{yi} + 2\zeta_i\omega_i\dot{q}_{yi} + \omega_i^2 q_{yi} = \frac{1}{M_i}\left[F_y(L,t)\phi_i(L) - M_x(L,t)\phi'_i(L)\right] \quad (8)$$

The moments, including the gyroscopic effect, are given as

$$M_x = I_d \sum \ddot{q}_{yi}\phi_i' + 2I_d \sum \dot{q}_{xi}\phi_i'\dot{\psi} \quad (9a)$$

$$M_y = I_d \sum \ddot{q}_{xi}\phi_i' + 2I_d \sum \dot{q}_{yi}\phi_i'\dot{\psi} \quad (9b)$$

where $\dot{\psi}$ is the rotor angular speed.

If a circular cross section is assumed for the flexible beam, then the natural frequencies, damping ratios, and vibration modes in the x and y directions will be the same, but the forces and moments in the x and y directions may differ.

The centrifugal force caused by the eccentric mass m_d of the disk is assumed to be acting as a concentrated force at the location $z=L$. The position vector of mass m_d with respect to the rotating frame Oxy is

$$\mathbf{r_G} = (x + e\cos\psi)\mathbf{i} + (y + e\sin\psi)\mathbf{j} \quad (10)$$

The acceleration of the disk can be found by taking the second derivative of equation (10) with respect to time as

$$\ddot{\mathbf{r}}_{\mathbf{G}} = \left(\ddot{x} - e\ddot{\psi}\sin\psi - e\dot{\psi}^2\cos\psi\right)\mathbf{i} + \left(\ddot{y} + e\ddot{\psi}\cos\psi - e\dot{\psi}^2\sin\psi\right)\mathbf{j} \quad (11)$$

When x and y components of the inertial force is substituted into the equations (8) and (9) the following equations are obtained.

$$\ddot{q}_{xi} + 2\zeta_i\omega_i\dot{q}_{xi} + \omega_i^2 q_{xi} = -\frac{m_d}{M_i}\left(\sum_j \phi_j(L)\ddot{q}_{xj} - e\ddot{\psi}\sin\psi - e\dot{\psi}^2\cos\psi\right)\phi_i(L) - \frac{I_d}{M_i}\left(\sum_j \phi'_j(L)\ddot{q}_{yj} + 2\sum_j \phi'_j(L)\dot{q}_{xj}\dot{\psi}\right)\phi'_i(L) \quad (12)$$

$$\ddot{q}_{yi} + 2\zeta_i\omega_i\dot{q}_{yi} + \omega_i^2 q_{yi} = -\frac{m_d}{M_i}\left(\sum_j \phi_j(L)\ddot{q}_{yj} + e\ddot{\psi}\cos\psi - e\dot{\psi}^2\sin\psi\right)\phi_i(L) - \frac{I_d}{M_i}\left(\sum_j \phi'_j(L)\ddot{q}_{xj} + 2\sum_j \phi'_j(L)\dot{q}_{yj}\dot{\psi}\right)\phi'_i(L) \quad (13)$$

Assuming only the first three modes for the solution, equations (12) and (13) can be written in a matrix form as

$$\mathbf{M}\ddot{\mathbf{q}} + \mathbf{C}\dot{\mathbf{q}} + \mathbf{K}\mathbf{q} = \mathbf{F} \quad (14)$$

where **M**, **C**, and **K** are respectively the mass, damping, and stiffness matrices while **F** is the force vector.

The generalized coordinates are given as $\mathbf{q} = \{q_{x1}, q_{x2}, q_{x3}, q_{y1}, q_{y2}, q_{y3}\}$, while their first and second derivatives are represented by vectors $\dot{\mathbf{q}}$ and $\ddot{\mathbf{q}}$, respectively.

The mass matrix is given by

$$\mathbf{M} = \begin{bmatrix} \mathbf{M}_1 & \mathbf{M}_2 \\ \mathbf{M}_2 & \mathbf{M}_1 \end{bmatrix} \quad (15)$$

where the sub-matrices are

$$\mathbf{M}_1 = \begin{bmatrix} 1+\mu\alpha_{11} & \mu\alpha_{12} & \mu\alpha_{13} \\ \mu\alpha_{21} & 1+\mu\alpha_{22} & \mu\alpha_{23} \\ \mu\alpha_{31} & \mu\alpha_{32} & 1+\mu\alpha_{33} \end{bmatrix} \quad (16)$$

$$\mathbf{M}_2 = \lambda\begin{bmatrix} \alpha'_{11} & \alpha'_{12} & \alpha'_{13} \\ \alpha'_{21} & \alpha'_{22} & \alpha'_{23} \\ \alpha'_{31} & \alpha'_{32} & \alpha'_{33} \end{bmatrix}. \quad (17)$$

Consequently, the *mass ratio*, μ, which is defined as the disk mass over shaft mass, is one of the important parameters for investigations and defined as

$$\mu = \frac{m_d}{m_s} \quad . \quad (18)$$

Another important parameter, the ratio of disk mass moment of inertia to the product of shaft-mass and shaft-length squared, is given as

$$\lambda = \frac{I_d}{m_s L^2} = \frac{1}{16}\frac{m_d}{m_s}\frac{D^2}{L^2} = \frac{1}{16}\mu\eta^2 \quad (19)$$

where the ratio of disk-diameter to shaft-length is another parameter to investigate, and given by

$$\eta = \frac{D}{L} \quad (20)$$

The damping coefficients matrix is given by

$$\mathbf{C} = \begin{bmatrix} \mathbf{C}_1 & 2\dot{\psi}\mathbf{M}_2 \\ -2\dot{\psi}\mathbf{M}_2 & \mathbf{C}_1 \end{bmatrix} \quad (21)$$

where $\mathbf{M}_2$ is the same as the sub mass matrix defined above and $\dot{\psi}$ is the angular speed of the shaft. $\mathbf{C}_1$ is defined as

$$\mathbf{C}_1 = diag([2\zeta_1\omega_1 \quad 2\zeta_2\omega_2 \quad 2\zeta_3\omega_3]) \quad (21)$$

where ζ_1, ζ_2, and ζ_3 are the damping ratios for the first, second and third modal vibrations.

The stiffness matrix is

$$\mathbf{K} = diag([\omega_1^2 \quad \omega_2^2 \quad \omega_3^2 \quad \omega_1^2 \quad \omega_2^2 \quad \omega_3^2]) \quad (22)$$

where ω_1, ω_2, and ω_3 are the first, second and third mode natural frequencies of the elastic beam.

The forcing term on the right hand side of the equation (14) can be obtained from

$$\mathbf{F} = \mu[\beta_1 f_x \quad \beta_2 f_x \quad \beta_3 f_x \quad \beta_1 f_y \quad \beta_2 f_y \quad \beta_3 f_y]^T \quad (23)$$

where

$$f_x = \ddot{\psi}\sin\psi + \dot{\psi}^2\cos\psi \quad (24)$$

$$f_y = -\ddot{\psi}\cos\psi + \dot{\psi}^2\sin\psi \quad (25)$$

In the equations, the generalized coordinates are divided by eccentricity e.

The other parameters used in the equations are defined as follows

$$\alpha_{ij} = \frac{\phi_i(L)\phi_j(L)}{\int_0^1 \phi_i^2(\xi)d\xi} \quad (26)$$

$$\alpha'_{ij} = \frac{\phi'_i(L)\phi'_j(L)}{\int_0^1 \phi_i^2(\xi)d\xi} \quad (27)$$

$$\beta_i = \frac{\phi_i(L)}{\int_0^1 \phi_i^2(\xi)d\xi} \quad (28)$$

where the dimensionless parameter ξ is defined as

$$\xi = \frac{z}{L} \quad (29)$$

The natural frequencies of a flexible cantilever (or fixed-free) beam are given

$$\omega_i = (\beta L)_i^2\sqrt{\frac{EI}{m_s L^4}} \quad (30)$$

where the values of βL for the first three modes are 1.875104, 4.694091, and 7.854757 [14]. The mode shapes of a flexible cantilever beam on the other hand are given as

$$\phi(\xi) = A\left[\sin\beta_i\xi - \sinh\beta_i\xi - \left(\frac{\sin\beta_i L + \sinh\beta_i L}{\cos\beta_i L - \cosh\beta_i L}\right)(\cos\beta_i\xi - \cosh\beta_i\xi)\right] \quad (31)$$

for $0 < \xi < 1$ [14].

The deflection of the rotor center in both x and y directions can be calculated from

$$x(L,t) = \sum_3 \phi_i(L)q_{xi}(t) \quad (32)$$

$$y(L,t) = \sum_3 \phi_i(L)q_{yi}(t) \quad (33)$$

and the whirl radius and whirl angle are calculated from

$$r(L,t) = \sqrt{x^2(L,t) + y^2(L,t)} \tag{34}$$

$$\theta(L,t) = \tan^{-1}\frac{y(L,t)}{x(L,t)} \tag{35}$$

To obtain a realistic transient behavior of the rotor whirl, rotor speed can be assumed to follow the following time function during run-up

$$\dot{\psi} = \omega_m(1 - e^{-\frac{t}{T}}) \tag{36}$$

and hence the angular acceleration

$$\ddot{\psi} = \frac{\omega_m}{T}e^{-\frac{t}{T}} \tag{37}$$

where ω_m is the maximum rotor speed, T is the time constant of the speed function. After a time of $4T$ rotor will reach 98% of its maximum speed.

3. SIMULATIONS

In the simulations, the density and the modulus of elasticity are taken to be ρ = 7700 kg/m^3 and E = 207 GPa, respectively. The shaft length and the shaft diameter are assumed to be L = 1 m and d = 0.01 m.

The equation (14) can also be written in a closed form such as

$$\begin{bmatrix}\dot{\mathbf{q}}\\ \ddot{\mathbf{q}}\end{bmatrix} = \begin{bmatrix}\mathbf{O} & \mathbf{I}\\ -\mathbf{M^{-1}K} & -\mathbf{M^{-1}C}\end{bmatrix}\begin{Bmatrix}\mathbf{q}\\ \dot{\mathbf{q}}\end{Bmatrix} + \begin{Bmatrix}\mathbf{O}\\ -\mathbf{M^{-1}F}\end{Bmatrix} \tag{38}$$

Then, the eigenvalues of the system can be calculated from the system matrix of

$$\mathbf{A} = \begin{bmatrix}\mathbf{O} & \mathbf{I}\\ -\mathbf{M^{-1}K} & -\mathbf{M^{-1}C}\end{bmatrix} \tag{39}$$

where **O** is the matrix of zeros and **I** is the identity matrix with appropriate dimensions.

For the classical Jeffcott rotor model, the natural frequencies of the rotor are calculated from

$$\omega_c = \sqrt{\frac{k_{eq}}{m_{eq}}} \tag{40}$$

where $k_{eq} = \frac{3EI}{L^3}$ and $m_{eq} = m_d + 0.23m_s$ [14]. The effect of shaft mass is added so as to assure not having a natural frequency of infinity for $\mu = \frac{m_d}{m_s} = 0$, which is the case of no disk on the shaft at all. The natural frequencies of the rotor with respect to the ratio of disk mass to shaft mass μ and the ratio of disk diameter to shaft length η are tabulated in Table 1.

Table 1. Natural frequencies of the rotor.

	μ = 1				μ = 10			
	ω_c	ω_1	ω_2	ω_3	ω_c	ω_1	ω_2	ω_3
η = 0.1	20.24	19.97	206.76	659.10	9.82	9.55	183.16	609.39
η = 0.3	20.24	18.19	170.39	578.43	9.82	7.52	87.90	479.71
η = 0.5	20.24	14.92	122.06	514.74	9.82	4.73	45.69	439.12
η = 0.7	20.24	11.13	88.42	481.62	9.82	2.81	33.84	424.17
η = 1.0	20.24	6.72	65.81	441.25	9.82	1.45	28.48	420.15

The natural frequencies of the flexible cantilever (or fixed-free) beam without a disk are computed as $\omega_{s1} = 45.58$ rad/s, $\omega_{s2} = 285.62$ rad/s, and $\omega_{s3} = 799.73$ rad/s for the given dimensions.

Figure 3 shows the first three natural frequencies of the rotor with respect to the mass ratio μ for different rotor diameter to beam length ratio η when the shaft speed $\dot{\psi}$ is 2000 rpm. It is preferred here to represent the changes in terms of the ratios of masses (μ) and dimensions (η=D/L) rather than using an inertia ratio (λ) since the inertia would be harder to visualize.

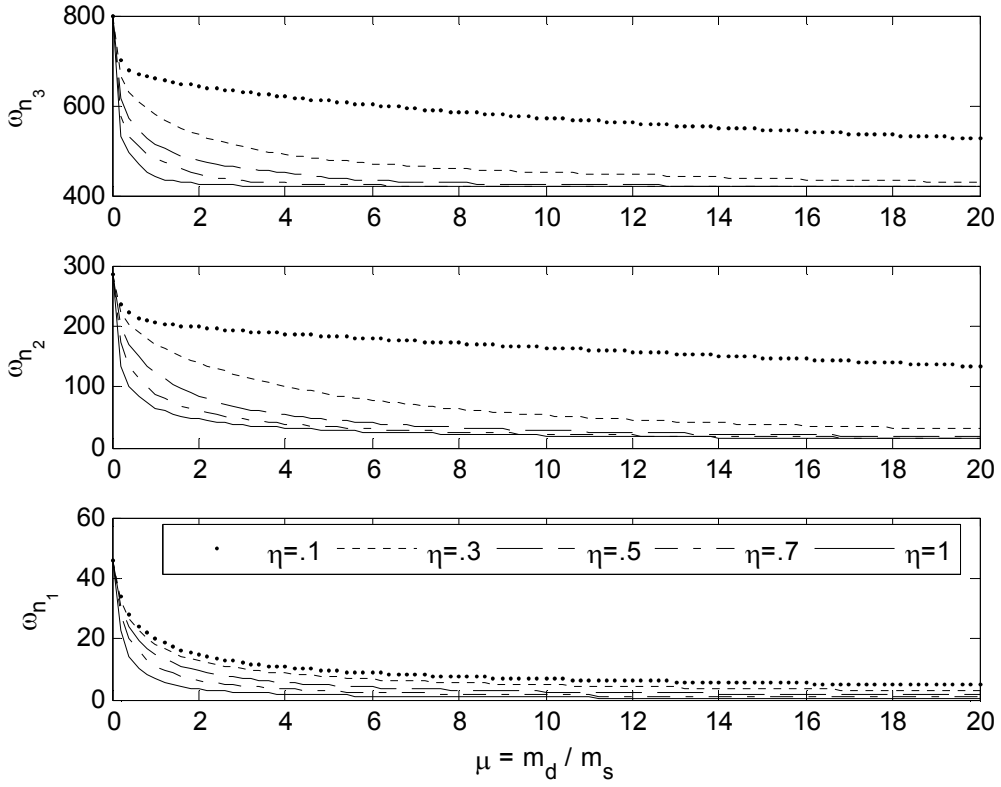

Figure 3. Natural frequencies of the rotor with respect to μ and η ($\dot{\psi} = 2000$ rpm).

When the mass ratio is zero, which is the case of no disk at all, all plots start from the natural frequencies of the flexible shaft. As the mass ratio increases, natural frequencies decrease, but the rate of decrease is comparatively low for higher values of mass ratio. All the first natural frequency curves obtained for different η values stay very close to each other. Although, the first natural frequency is not affected by the *D*/*L* ratio for increasing values of mass ratio μ, the second and third natural frequencies are observed to be affected with these parameters.

Another remarkable observation is the instability of the system for higher values of μ and/or η, which are mainly due to the disk inertia and dimension. For larger values of aforementioned parameters, some of the eigenvalues of the system become real and positive so as to make the system dynamics unstable. Figure 4 shows the stable and unstable regions for the selection of μ and η. Obviously system is stable for relatively smaller values of both parameters, and hence safe to operate in this region.

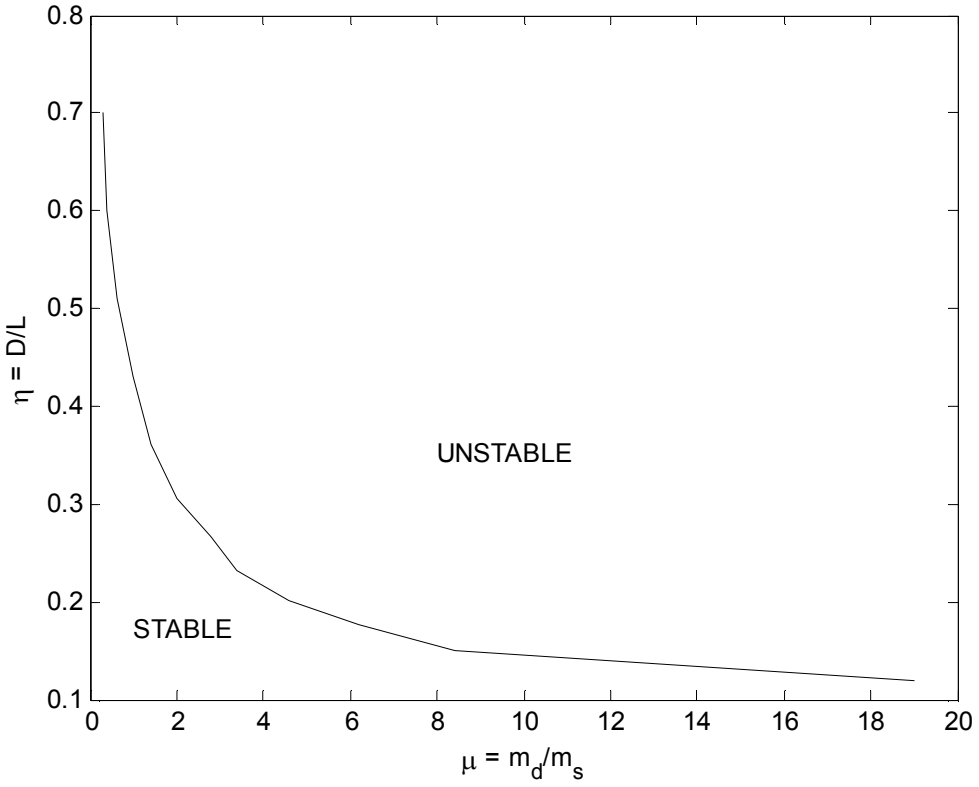

Figure 4. Stable and unstable regions for a range of μ and η values.

To show the difference between the first natural frequency of the continuous shaft-rotor system and the natural frequency of the classic Jeffcott rotor model, which can be calculated from equation (40), the percent errors are depicted in Figure 5 for increasing mass ratio. Jeffcott rotor model generally predicts natural frequencies higher than the continuous shaft-disk model for all mass ratios. While this error is very small for all values of η for small μ, it gets much larger for higher values of μ. This is basically due to the fact that Jeffcott is a very simple approximation of the problem and the Jeffcott model does not have the ability to reflect neither of the flexible beam theory and gyroscopic effects.

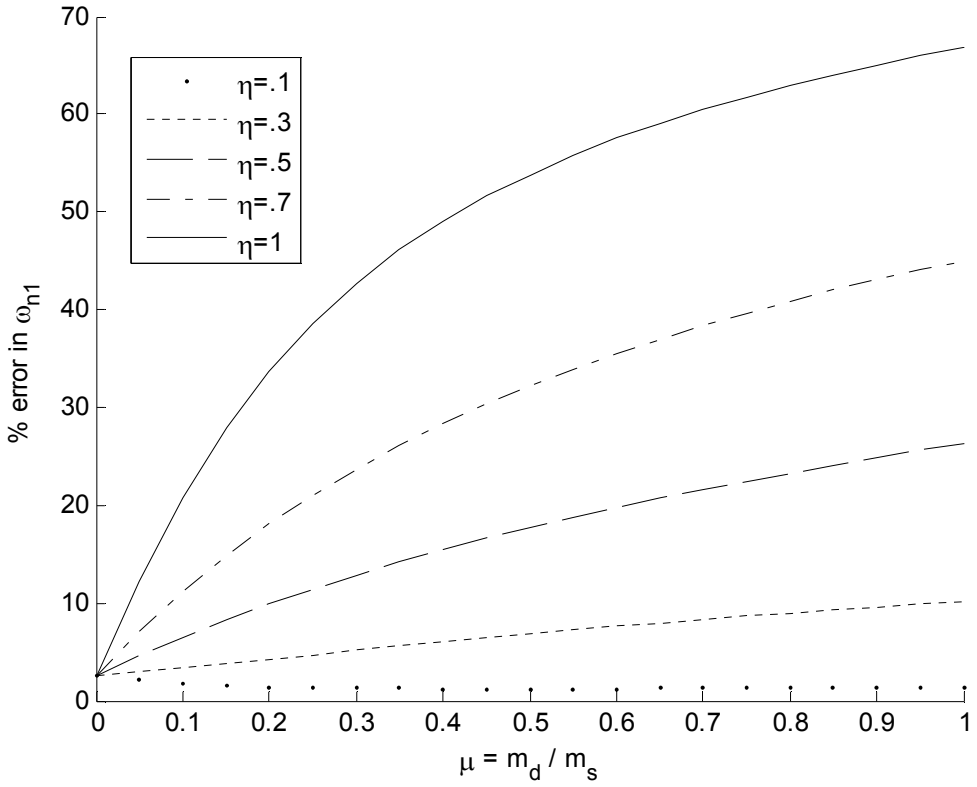

Figure 5. Percent error plots for the first natural frequency of the continuous shaft-disk system.

4. CONCLUSIONS

This paper develops the model of a disk mounted on a continuous flexible-cantilever beam by extending the classical Jeffcott rotor model to the first three modes of the continuous shaft-disk system, which is not possible through the classical Jeffcott rotor model. Equations of motion are developed by using the normal modes of a constrained structure method with the assumption that the inertial force and moment created by the rotating disk having mass unbalance are the constraints for the continuous beam. The results were compared with the classical one and shown to be quite different with the inclusion of flexible beam theory and gyroscopic effects.

There are two important parameters of the model: The first one is the mass ratio which is defined as the disk-mass over the shaft-mass. The second parameter is the ratio of disk-diameter to shaft-length. The effects of all these parameters on stability of the rotor-shaft system are investigated and presented in the paper.

Current model predicts the first natural frequency very close to the one obtained from the classical Jeffcott rotor model for lower ratios of mass and dimension. However it increases with increasing these two ratios; especially with the increase of η, the dimensional ratio. Beyond the first mode, the model presented in this study correctly predicts second and third natural frequencies of the system, which can be easily extended to find natural frequencies higher than the third one.

Another important finding is the possibility of determining the stability of the system, which is not also possible through the classical Jeffcott rotor model. By defining eigenvalues of the system one can decide if the system is unstable. The system under investigation was found to be undergoing to an unstable motion for increasing inertia of the disk.

REFERENCES

[1] Nelson, F.C., "A brief history of early rotor dynamics", ***Sound and Vibration***, 37 (6): 8-11, (2003).

[2] Nelson, F.C., "Rotor dynamics without equations", ***International Journal of COMADEM***, 10 (3): 2-10, (2007).

[3] Rao, J.S., "History of Rotating Machinery Dynamics", ***Springer Science + Business Media***, New York, NY, (2011).

[4] Rao , J. S., "Rotor Dynamics", ***John Wiley and Sons***, (1983).

[5] Vance, J. M., "Rotordynamics of Turbomachinery", ***John Wiley and Sons***, New York, NY, (1988).

[6] Kramer, E., "Dynamics of Rotors and Foundations", Springer –Verlag, (1993).

[7] Genta, G., "Dynamics of Rotating Systems", ***Springer Science+Business Media***, New York, NY, (2005).

[8] Vance, J., Zeidan, F., Murphy, B., "Machinery Vibration and Rotordynamics", ***John Wiley and Sons***, New Jersey, (2010).

[9] Genta, G., "Whirling of unsymmetrical rotors: A finite element approach based on complex co-ordinates", ***Journal of Sound and Vibration***, 124 (1): 27-53, (1988).

[10] Kessler, C. L., "Complex modal analysis of rotating machinery", PhD thesis, University of Cincinnati, (1999).

[11] Campos, J., Crawford, M., Longoria, R., "Rotordynamic Modeling Using Bond Graphs: Modeling the Jeffcott Rotor", ***IEEE Transaction on Magnetics***, 41 (1):274-280 (2005).

[12] Khanlo, H.M., Ghayour, M., Ziaei-Rad, S., "Chaotic vibration analysis of rotating, flexible, continuous shaft-disk system with a rub-impact between the disk and the stator", ***Commun Nonlinear Sci Numer Simulat***, 16: 566-582, (2011).

[13] Thomson, W.T., "Theory of Vibration with Applications", ***Prentice Hall***, Englewood Cliffs, NJ, (1981).

[14] Rao, S.S., "Mechanical Vibrations", ***Prentice Hall***, New Jersey, (2005).